Xiaopeng Bi, Zhiwei Sun, Timothy Lau, Zeyad Alwahabi and Graham Nathan
Simultaneous planar measurements of gas and particle velocities in particle-laden flows: proof-of-concept
Proceedings of the 22nd Australasian Fluid Mechanics Conference (AFMC2020), 2020 / pp.1-4

Published at: https://doi.org/10.14264/9eb1c68

22nd Australasian Fluid Mechanics Conference AFMC2020
Brisbane, Australia, 7-10 December 2020
https://doi.org/10.14264/9eb1c68

Simultaneous planar measurements of gas and particle velocities in particle-laden flows: proof-of-concept

Xiaopeng Bi[1,2], Zhiwei Sun[1,2], Timothy Lau[1,2], Zeyad Alwahabi[1,3] and Graham Nathan[1,2]

[1]Centre for Energy Technology, The University of Adelaide, Adelaide SA 5005, Australia

[2]School of Mechanical Engineering, The University of Adelaide, Adelaide SA 5005, Australia

[3]School of Chemical Engineering and Advanced Materials, The University of Adelaide, Adelaide SA 5005, Australia

Abstract

A laser-based technique is reported, employing simultaneous laser-induced fluorescence (LIF) and phosphorescence (LIP) to respectively mark the gas- and particle- phases and allow their simultaneous velocity measurement in a particle-laden flow. The technique discriminates the phases by optically separating the fluorescent and phosphorescent signals from each other and also from the scattering signals, thorough the novel use of optical filters and temporal separation. A proof-of-concept demonstration was conducted with using 250 μm PMMA spherical particles and 4 μm BAM:Eu^{2+} phosphorescent tracers, suspended in a water cuvette. Under 355 nm excitation (3rd harmonic of the Nd:YAG laser), both PMMA fluorescent and BAM:Eu^{2+} phosphorescent signals are shown to be sufficiently strong for imaging with CCD cameras, and sufficiently separable with using spectral filters and temporal profiles.

Keywords

Laser diagnostics; particle-laden flows; experimental methods; fluid velocity; particle velocity.

Introduction

Simultaneous measurement of gas- and particle- phase velocities is of vital importance to advance understanding of the complex interactions between the two phases in particle-laden flows. This understanding is important because the instantaneous gas-particle distributions can influence phenomena such as mass transport, ignition, combustion, heat transfer, chemical reactions and dust diffusion [4, 5, 15, 16], which in turn have significant effects on thermal efficiencies and pollutant emissions within the many industrial systems involve the use of particles. This paper presents a proof-of-concept of a method to enable measurements of the velocity field of both phases within time-frames that are short relative to any fluid time-scales utilising laser-induced fluorescence and phosphorescence.

The conventional method to non-intrusively measure the velocity in turbulent flows is particle image velocimetry (PIV), which relies on measuring the scattered laser light from particles and flow tracers. However, in typical particle-laden flows, the particle diameters are O(10) μm or more, while the tracers are O(1) μm or less [12, 13, 20, 22]. It is therefore challenging to discriminate between the scattered signal from the particles and tracers, as is needed for simultaneous measurement, as the scattering intensity is proportional to the square of particle diameter [8, 17]. That is, the major limitation of conventional PIV is that the signals from spatially-close large particles and tracers are difficult to be discriminated since they have the same wavelength and occur at the same time as the excitation laser.

Previously, many different methods have been developed to reduce the cross-interference between particles and tracers, such as establishing a thresholding between phases [19], applying an object-growing algorithm [18], using the median-filter [9] or the Wiener filter [4] in image processing, utilising a spectral atomic filter or developing very-high-resolution PIV systems [22]. While these methods have improved the conventional PIV technique, they also exhibit limitations, such as still yielding some cross-interferences, requiring expensive processing cost or requiring complicated experiments. Therefore, there are significant limitations in the extent to which the signals from the carrier- and particle- phase can be separated with the sole use of scattering as the optical detection method.

Laser-induced fluorescence (LIF) and phosphorescence (LIP), are common laser diagnostic techniques that have a wide range of applications [1-3, 10, 14], partly because a range of phosphor particles and fluorescent tracers are available with different emission spectra and temporal profiles. In particular, thermographic phosphor particles have recently been used to conduct simultaneous measurements of gas velocity and temperature in a turbulent flows, both relying on phosphorescent signals [6, 21]. While this study demonstrates that it is viable to use luminescent signals for velocity measurements, as yet there is no study that has demonstrated the optical discrimination between the signals from different LIF/LIP particles to allow their simultaneous velocity measurements in a particle-laden flow.

This paper presents the first step towards developing a non-intrusive, simultaneous, planar measurements of fluid- and particle- phase velocities that can be applied to a range of flows, including turbulent particle-laden flows. In particular, this study aims to demonstrate the proof-of-concept of a laser-based technique to discriminate the luminescent signals from both the particles and fluid tracers. This is demonstrated by conducting measurements of the fluorescence of PMMA particles and phosphorescence of BAM:Eu^{2+} tracers suspended in a water cuvette.

Methodology

The experiment consisted of simultaneous measurements of fluorescence and phosphorescence of particles and tracers seeded and suspended in water within a cuvette, as shown in Figure 1. The cuvette is made from UV fused quartz with a transmission rate of light wavelength between 300 nm and 1000 nm over 85 %. The size of the cuvette was 10 mm × 10 mm × 43 mm, and it was completely filled with distilled water and particles.

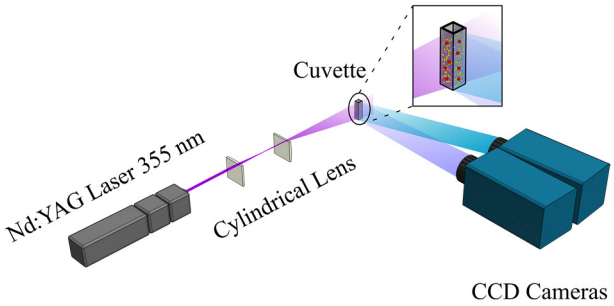

Figure 1: Schematic diagram of the experimental arrangement. The experiment consists of measurements of LIP and LIF from tracers and particles, respectively, within a water cuvette. The source of illumination was a single pulsed Nd:YAG laser operating at 355 nm, while two separate CCD cameras were used to measure LIF and LIP.

The particles consisted of polymethyl methacrylate (PMMA, Microbeads Dynoseeds) of mean diameter of 250 µm. These particles are spherical in shape and have a mono-dispersed size distribution (standard deviation of the particle size under 5%). These properties of PMMA particles offer significant advantages for fundamental studies of particle-laden flows because the relatively isotropic homogeneous property avoids in-situ measurements of particle size and shape, which further provides a favourable potential for systematic studies of different non-linear coupled flow effects.

$BaMgAl_{10}O_{17}:Eu^{2+}$, also called BAM:$Eu^{2+}$ phosphor particles (KEMK63/F-P1, Phosphor Technology, median diameter of 4 µm) were used as fluid "tracers". These tracers have a non-spherical shape, with the phosphorescence emission peak of approximately 455 nm and emission signal lifetime of ~1 µs at room temperature under laser excitation of 355 nm [3, 7].

A Quantel Brilliant B single pulsed Nd:YAG laser operated at the power of approximately 5 mJ and a pulsing frequency of 10 Hz was used to deliver a laser light with wavelength of 355 nm (3^{rd} harmonic) and thickness of approximately 400 µm for simultaneously exciting both the PMMA particles and BAM:Eu^{2+} tracers in the cuvette. A pair of cylindrical lens (f = 500 mm and f = 1000 mm) was aligned to modify the laser light into a vertically diverged laser sheet posting on the middle plane of the cuvette side face.

Two CCD cameras (PCO.2000) were used to image the particles and tracers within the cuvette. Table 1 summarises the details of imaging arrangement for each detection channel. Channel 1 was specially designed for only capturing BAM:Eu^{2+} LIP signals with applying a triggering delay time of 50 ns relative to laser pulse time on the related camera and using the long-pass optical filter of 409 nm (Semrock LP409). This only transmits the signals of wavelength larger than 409 nm, to block scattered interference and PMMA LIF. Channel 2 was specifically equipped with a band-pass optical filter (Semrock 390 ± 18 nm) to transmit the "instantaneous" PMMA LIF signals located at the spectra wavelength between 372 nm and 408 nm, whilst blocking the majority of the interferences from scattering and BAM:Eu^{2+} LIP. The exposure time of both cameras were 1000 ns, while Channel 2 for PMMA LIF signals was triggered earlier (950 ns before the laser pulse) such that the camera temporal gate is timed to transmit the "instantaneous" laser-induced signals. However, Channel 1 for BAM:Eu^{2+} LIP signals was triggered 50 ns after the laser pulse to avoid collecting the "prompt" response. Both cameras were aligned to image the same region consisting of 6 mm × 14 mm at a resolution of 28.20 pixels per millimetre. Both were also synchronised with the laser using a digital delay generator (DG535) to respectively capture the signals of BAM:Eu^{2+} LIP and PMMA LIF. The image pairs from the two cameras were spatially aligned by matching points on a target image consisting of a grid with a spacing of 3.55 mm illuminated with room light.

Detection channels	No. 1	No. 2
Objective signals	BAM:Eu^{2+} LIP	PMMA LIF
CCD cameras	PCO. 2000 (1)	PCO. 2000 (2)
Lens	Tamron 70-200 F/2.8	Cerco UV 100 F/2.8
Filters	LP409 Semrock	BP390 (BP18) Semrock
Exposure time (ns)	1000	1000
Delay to laser (ns)	+50	-950

Table 1: Imaging arrangement for separately capturing LIP and LIF.

Results

Figure 2 presents the prompt emission spectrum of PMMA particles and the temporally delayed spectrum of BAM:Eu^{2+} tracers suspended in water and under 355 nm excitation, separately measured by using a SpectraPro-500i spectrometer (Princeton Instruments). Although the emission spectrum of BAM:Eu^{2+} ranging from 400 nm to 520 nm has been well-known to the phosphor thermometry community [3, 7], that of PMMA has rarely been reported, showing a broadband distribution up to the green spectral region. Specifically, the results show that in the spectral region between 360 nm and 395 nm, the emission signal intensity ratio, defined as the emission signal intensities normalised by their peak values, of PMMA is approximately 0.7, whereas that of BAM:Eu^{2+} is close to zero. That is, imaging at this spectral region allows measurements of the LIF signal of PMMA particles without receiving the LIP of BAM:Eu^{2+} tracers.

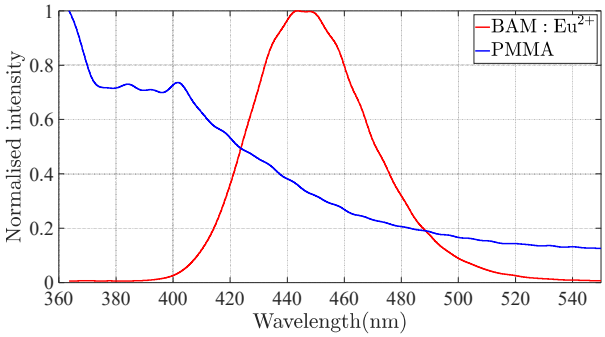

Figure 2: Laser-induced emission spectra of BAM:Eu^{2+} tracers and PMMA particles under a laser excitation wavelength of 355 nm. The intensities of both spectra have been respectively normalised by their peak values. The emitted spectrum of BAM:Eu^{2+} was recorded after 50 ns delay of the laser pulse, while the PMMA emitting signals were recorded without delay.

The results presented in Figure 2 also show that the spectral band where the BAM:Eu^{2+} phosphorescence is the strongest, i.e. between 410 nm and 500 nm, also includes a spectral region where PMMA fluorescence is strong. However, the PMMA fluorescence lifetime is expected to be small, on the order of a few nanoseconds or less, while the phosphorescence lifetime of BAM:Eu^{2+} is approximately 1 µs [3, 7]. Hence, the phosphorescent signal was separated from the fluorescent signal by applying a time delay of 50 ns relative to the laser pulse for the Camera 1 recording the LIP signal (see also Table 1). It should also be noted that the lifetime of both PMMA fluorescence and BAM:Eu^{2+} phosphorescence is short relative to the fluid time-scales, which ensures that any "streaks" are

negligible. Therefore, where combined with the appropriate imaging configuration, as is presented here, PMMA and BAM:Eu^{2+} form a strong candidate pair for simultaneous phase discrimination in particle-laden flows.

Figure 3 presents simultaneous measurements of LIP (left column) and LIF (right column), for the case where the flow was seeded with both PMMA particles and BAM:Eu^{2+} tracers (3rd and 4th rows), PMMA particles only (1st row) and BAM:Eu^{2+} tracers only (2nd row). The first three rows were recorded using temporal separation settings as summarised in Table 1, while the bottom row was recorded without any triggering delay in either camera. It can be seen that from Figure 3b, where the flow is seeded only with PMMA particles, that the PMMA particles are typically large, approximately 7 pixels in diameter. Furthermore, the LIF signal from PMMA particles is strong, typically thousands of counts, even without the use of an intensifier. In contrast, the PMMA LIF interference in the LIP camera is so weak, that it is, almost indistinguishable from the noise (see figure 3a). This demonstrates that the choice of the optical filter and triggering delay (as summarised in Table 1) sufficiently removes LIF and scattering interferences from the LIP imaging, while also allowing a sufficiently strong LIF signal into the LIF camera.

Figure 3c and Figure 3d, on the other hand, show that the LIP signal from the BAM:Eu^{2+} tracers are only observed in the LIP camera, and not in the LIF camera. Furthermore, the LIP signal in the former camera is strong, in excess of 10,000 counts, with the tracers appearing as "small" particles on the order of 1 pixel in diameter. Figure 3e and Figure 3f present images of the flow seeded with both PMMA particles and BAM:Eu^{2+} tracers. As expected, images of the small BAM:Eu^{2+} tracers are only observed in the LIP camera, while images of the large PMMA particles are only observed in the LIF camera. The signal strength also remains strong, peaking at ~13,000 counts for the former and ~7,000 counts for the latter. Considering the noise level on both cameras are <300, this results in a signal-to-noise ratio of >23. The clear imaging of distinct particles and the tracers also implies that the images are suitable for cross-correlation, i.e., the images can be used to obtain the velocity field where double-pulsed imaging is utilised.

In contrast, in the case where images of both PMMA particles and BAM:Eu^{2+} tracers were recorded without any camera triggering delay (Figure 3g and Figure 3h), the results have shown that there is substantial "optical leakage" of the PMMA LIF signal into the LIP camera. That is, the use of camera delay is required to enable sufficient discrimination between the cases, at least for the particles and tracers chosen in the current experiment.

It is also interesting to note that phosphor tracers, including BAM:Eu^{2+} are commonly used to measure temperature [7, 11]. Therefore, the present method can be plausibly extended to provide fluid temperature measurements simultaneously with the particle and fluid velocity fields utilising the previously-developed phosphor thermometry method.

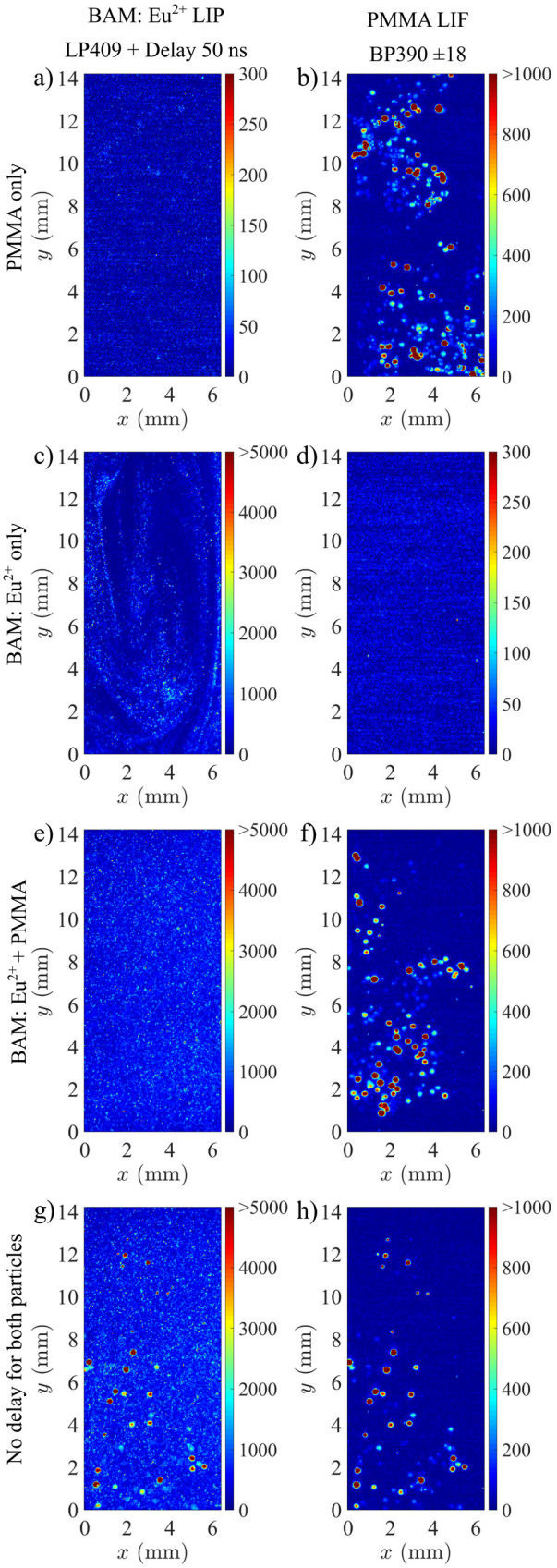

Figure 3: Simultaneous images of LIP (left column) and LIF (right column) of a water flow suspended with both PMMA particles and BAM:Eu^{2+} tracers (3rd and 4th rows), PMMA particles only (1st row) and BAM:Eu^{2+} tracers only (2nd row). The six images within the first three rows were captured by a pair of CCD cameras employing both wavelength and temporal discrimination as summarised in Table 1, while in the bottom row, no triggering delay was used in both cameras to demonstrate the imaging of both particles (Figure 3.g).

Conclusion

A laser-based method to discriminate between the particle phase and the fluid phase has been successfully demonstrated utilising laser-induced fluorescence and laser-induced phosphorescence, together with optical filtering, camera triggering delay and the selection of PMMA and BAM:Eu^{2+} as the particles and tracers, respectively. The results show that, not only can the two phases be clearly separated, but also that the signal strength of both the LIF and LIP signals are sufficiently strong that they can be captured by non-intensified CCD cameras, with a signal-to-noise ratio greater than 23. Furthermore, the captured images were found to be of sufficient quality and fidelity that they can be used to obtain the velocity field where double-pulsed imaging is employed.

Acknowledgments

The authors gratefully acknowledge the internationally financial contributions from the U.S. Department of Energy, Sandia National Laboratories through the Gen 3 Particle Pilot Plant (G3P3): Integrated High-Temperature Particle Receiver System for CSP (1697-1503) and the Australian government through the Australian Research Council (Discovery Grant DP180102045) and the Australian Renewable Energy Agency (Grant 2015/RND054).

References

[1] Abram, C., Fond, B., Heyes, A.L., and Beyrau, F., (2013). High-speed planar thermometry and velocimetry using thermographic phosphor particles. *Applied Physics B*, 111(2), 155-160.

[2] Abram, C., Fond, B., and Beyrau, F., (2018). Temperature measurement techniques for gas and liquid flows using thermographic phosphor tracer particles. *Progress in energy and combustion science*, 64, 93-156.

[3] Aldén, M., Omrane, A., Richter, M., and Särner, G., (2011). Thermographic phosphors for thermometry: a survey of combustion applications. *Progress in energy and combustion science*, 37(4), 422-461.

[4] Becker, L.G., von Langenthal, T., Pielsticker, S., Böhm, B., Kneer, R., and Dreizler, A., (2019). Experimental investigation of particle-laden flows in an oxy-coal combustion chamber for non-reacting conditions. *Fuel*, 235, 753-762.

[5] Cassel, H. and Liebman, I., (1959). The cooperative mechanism in the ignition of dust dispersions. *Combustion and Flame*, 3, 467-475.

[6] Fan, L., Gao, Y., Hayakawa, A., and Hochgreb, S., (2017). Simultaneous, two-camera, 2D gas-phase temperature and velocity measurements by thermographic particle image velocimetry with ZnO tracers. *Experiments in Fluids*, 58(4), 34.

[7] Fond, B., Abram, C., and Beyrau, F., (2015). Characterisation of the luminescence properties of BAM: Eu^{2+} particles as a tracer for thermographic particle image velocimetry. *Applied Physics B*, 121(4), 495-509.

[8] Kalt, P.A.M. and Nathan, G.J., (2007). Corrections to facilitate planar imaging of particle concentration in particle-laden flows using Mie scattering. Part 2: diverging laser sheets. *Applied optics*, 46(29), 7227, DOI: 10.1364/AO.46.007227.

[9] Kiger, K.T. and Pan, C., (2000). PIV technique for the simultaneous measurement of dilute two-phase flows. *Journal of Fluids Engineering*, 122(4), 811-18, DOI: 10.1115/1.1314864.

[10] Kueh, K.C., Lau, T.C., Nathan, G.J., and Alwahabi, Z.T., (2017). Single-shot planar temperature imaging of radiatively heated fluidized particles. *Optics Express*, 25(23), 28764-28775.

[11] Kueh, K.C., Lau, T.C., Nathan, G.J., and Alwahabi, Z.T., (2018). Non-intrusive temperature measurement of particles in a fluidised bed heated by well-characterised radiation. *International Journal of Multiphase Flow*, 100, 186-195.

[12] Lau, T.C. and Nathan, G.J., (2016). The effect of Stokes number on particle velocity and concentration distributions in a well-characterised, turbulent, co-flowing two-phase jet. *Journal of Fluid Mechanics*, 809, 72-110.

[13] Lau, T.C.W., Frank, J.H., and Nathan, G.J., (2019). Resolving the three-dimensional structure of particles that are aerodynamically clustered by a turbulent flow. *Physics of Fluids*, 31(7), 071702, DOI: 10.1063/1.5110323.

[14] Lewis, E.W., Lau, T.C., Sun, Z., Alwahabi, Z.T., and Nathan, G.J., (2020). Luminescence interference to two-colour toluene laser-induced fluorescence thermometry in a particle-laden flow. *Experiments in Fluids*, 61(4), 1-16.

[15] Longmire, E.K. and Eaton, J.K., (1992). Structure of a particle-laden round jet. *Journal of Fluid Mechanics*, 236, 217-257.

[16] Nathan, G., Mi, J., Alwahabi, Z., Newbold, G., and Nobes, D., (2006). Impacts of a jet's exit flow pattern on mixing and combustion performance. *Progress in energy and combustion science*, 32(5-6), 496-538.

[17] Olsen, M.G. and Adrian, R.J., (2000). Out-of-focus effects on particle image visibility and correlation in microscopic particle image velocimetry. *Experiments in Fluids*, 29(1), S166-S174, DOI: 10.1007/s003480070018.

[18] Paris, A. and Eaton, J.K., (1999). Measuring velocity gradients in a particle-laden channel flow. in *Proceedings of the Third International Workshop on Particle Image Velocimetry*, Santa Barbara, 513-18.

[19] Sakakibara, J., Wicker, R.B., and Eaton, J.K., (1996). Measurements of the particle-fluid velocity correlation and the extra dissipation in a round jet. *International Journal of Multiphase Flow*, 22(5), 863-881, DOI: 10.1016/0301-9322(96)00014-6.

[20] Sheen, H.J., Jou, B.H., and Lee, Y.T., (1994). Effect of particle size on a two-phase turbulent jet. *Experimental Thermal and Fluid Science*, 8(4), 315-327, DOI: 10.1016/0894-1777(94)90061-2.

[21] Someya, S., Okura, Y., Uchida, M., Sato, Y., and Okamoto, K., (2012). Combined velocity and temperature imaging of gas flow in an engine cylinder. *Optics Letters*, 37(23), 4964-4966.

[22] Tanaka, T. and Eaton, J.K., (2010). Sub-Kolmogorov resolution partical image velocimetry measurements of particle-laden forced turbulence. *Journal of Fluid Mechanics*, 643, 177-206, DOI: 10.1017/S0022112009992023.